One-year plasma *N*-linked glycome intra-individual and inter-individual variability in the chicken model of spontaneous ovarian adenocarcinoma

R. Brent Dixon[a], Michael S. Bereman[a], James N. Petitte[b], Adam M. Hawkridge[a], David C. Muddiman[a,*]

[a] W.M. Keck FT-ICR Mass Spectrometry Laboratory, Department of Chemistry, North Carolina State University, Raleigh, NC 27695, USA
[b] Department of Poultry Science, North Carolina State University, Raleigh, NC 27695, USA

ARTICLE INFO

ABSTRACT

Spontaneous epithelial ovarian cancer (EOC) in the chicken presents a similar pathogenesis compared with humans including CA-125 expression and genetic mutational frequencies (*e.g.*, p53). The high prevalence of spontaneous EOC chickens also provides a unique experimental model for biomarker discovery at the genomic, proteomic, glycomic, and metabolomic level. In an effort to exploit this unique model for biomarker discovery, longitudinal plasma samples were collected from chickens at three-month intervals for one year. The study described herein involved cleaving the *N*-glycans from these longitudinal chicken plasma samples and analyzing them via nanoLC–FTMS/MS. Glycans identified in this study were previously found in human plasma and this work provides a promising methodology to enable longitudinal studies of the *N*-linked plasma glycome profile during EOC progression. The structure, abundance, and intra-variability and inter-variability for 35 *N*-linked glycans identified in this study are reported. The full potential of the chicken model for biomarker discovery has yet to be realized, but the initial interrogation of longitudinally-procured samples provides evidence that supports the value of this strategy in the search for glycomic biomarkers.

1. Introduction

It is an accepted concept that animal models of human disease are an invaluable asset in the development, pathologic morphology, and response to therapeutic treatment of disease [1]. These models aid in the understanding of disease etiology and pathologic progression at an accelerated and accessible rate. Animal models of disease can provide evidence in clinical research as to whether certain treatment options are effective in bringing about remission of cancers or other illnesses. Common examples of animal models that aid in the study of human disease etiology, progression, and treatment therapies are the chicken [2,3], zebra fish (*Danio rerio*) [4], dog [5], mouse [6–8], rabbit [9], and monkey [10]. Recent work has been devoted to the study of the chicken (*Gallus domesticus*) as a potential animal model for human epithelial ovarian cancer (EOC) [11]. Briefly, the incessant ovulation hypothesis [12], along with the expression of CA-125 [13,14], and the correlation of p53 tumor suppressor gene mutation and other oncogenes [15] (*i.e.*, ras and HER2/neu) similar to human give reasonable evidence to develop this model. This work presents data demonstrating that the cleaved *N*-linked glycans identified from plasma have the same composition whether their origin is from chickens or humans. The availability of these chicken samples for longitudinal sampling has enabled this subset of the entire sample cohort for the intra-variability and inter-variability of *N*-linked glycans to be studied.

Glycosylation of proteins play key roles as a regulator for many biochemical processes such as cellular signaling, division, adhesion, protein folding, stability and disease. Generally, glycans are categorized as either *O*-linked to serine or threonine or *N*-linked to asparagine residues on approximately 50% of gene products [16]. Glycosylation is highly sensitive to its cellular environment [17] and aberrant protein glycosylation is known to occur in various diseases [17–20]. The association of deregulated uptake of glucose in cancer was first described by Warburg starting in the 1920s [21]. Wu et al. were the first to correlate this increase in glucose uptake to protein post-translational modification when they observed that larger membrane glycoproteins occur in cancerous fibroblasts as compared to healthy fibroblasts [22]. Rostenberg et al. pursued this implication further and reported that glycosylation patterns were altered in alpha-1-antitrypsin in several cancers [23]. In the 1980s, Gehrke and coworkers linked glycan abundance to ovarian and lung carcinomas by gas–liquid chromatography (GLC) [24]. Recent research continues to emphasize that glycosylation has a signifi-

* Corresponding author at: W.M. Keck FT-ICR Mass Spectrometry Laboratory, Department of Chemistry, North Carolina State University, 2620 Yarbrough Drive, Dabney Hall CB 8204, Raleigh, NC 27695, USA. Tel.: +1 919 513 0084; fax: +1 919 513 7993.
    E-mail address: david_muddiman@ncsu.edu (D.C. Muddiman).

cant role in the progression of human carcinomas and as a potential biomarker [17,20,25–31]. For example, it has been reported that sialylation of glycoproteins is altered between normal and malignant conditions [17,32,33]. This has led to numerous studies of glycans cleaved from glycosylated proteins endogenous to biological matrices (e.g., serum or plasma). In addition, there are reports which attribute an increase in the size and branching of N-linked glycans characteristic of cancer cells to an increase in activity of various glycotransferases [34,35]. These observations stimulated subsequent studies that reported similar unique glycan structures as putative molecular markers of cancer in several tissues including prostate [32,36,37], liver [38], breast [39,40], and ovary [41,42]. Oligosaccharides associated with the current EOC clinical marker CA-125 have also been characterized [43]. Furthermore, the importance of post-translational modifications in the context of cancer has been recently reviewed [44].

In birds, as in mammals, oligosaccharides are synthesized in the ER-Golgi pathway where glycotransferases are localized. Often, the expression of glycotransferases and the glycosylation of proteins are developmentally regulated and cell-type specific. Likewise, glycosylation moieties can be cell-type specific. Nevertheless, protein glycosylation in birds share significant similarities with that observed for human proteins. Comparative glycosylation of immunoglobulins has revealed interesting and significant commonalities between the domestic fowl and human patterns of oligoscaccharides [45]. Terminal sialylation and galactosylation of human and chicken IgG appears to be similar. Analysis of neutral sugar content between human, several mammals (pig, cow sheep, mouse, rat, dog, cat), rhesus monkey serum IgG, and chicken serum IgG(IgY) revealed variation in total neutral sugars/protein but only chicken and human shared one form of sialic acid residues, suggesting a similar distribution between human and chicken [45]. None of the other species matched the human composition in this regard. Differences were found between chicken and human in the presence of high mannose type N-linked oligosaccharides in chicken IgG, while all forms of human complex type N-linked oligosaccharides were represented in chicken. Finally, human and chicken acidic oligosaccharides contain exclusively the sialic acid form N-acetylneuraminic acid (NANA) while other species contained various proportions of NANA and N-glycolylneuraminic acid (NGNA) [45]. This latter feature is biologically important. Terminal structures on the cell surface in the form of sialic acids are involved in intercellular function and "cross-talk". The fact that humans and chickens contain exclusively NANA has suggested that avian glycosylation patterns would be less immunogenic to human.

In addition to immunoglobulins, other studies have suggested conserved glycan species on the cell surface of avian tissue. The major N-linked glycans of the chick brain synaptic plasma membrane appear to be highly conserved, particularly neutral glycans, such as oligomannosidic structures, LewisX, core-fucose, and bisecting GlcNAc [46]. The conservation of glycosylation patterns in avian tissues is best reflected in the efforts to produce human recombinant, biologically active, therapeutic proteins in chicken embryos and eggs. Recombinant human lactoferrin produced in chick embryo allantoic fluid has a similar glycosylation, while the glycosylation of human lactoferrin in the milk of transgenic mice was found to be highly modified [20,47]. Likewise, transgenic hens that were developed to produce human interferon in their eggs generated recombinant protein with a major glycoform found in naturally occurring human interferon [48]. Taken together, it is reasonable to expect that the glycosylation profiles of avian ovarian carcinomas will also yield biologically significant results that are applicable to or provide insight to the secreted glycoprotein changes associated with human tumors.

A large-scale collection of longitudinal plasma samples from 239 chickens over a one-year period recently concluded resulting in a substantial biorepository for early-stage EOC biomarker discovery. A recently developed plasma N-linked glycan assay for nLC-LTQ–FT MS [49] was used in this study to interrogate the longitudinal sample sets from four birds out of the original 239. Out of the four birds, two were assessed to be healthy, one had early-stage EOC, and one had advanced EOC or oviductal cancer (OVD). A total of 35 N-linked glycans cleaved from the 4 longitudinal plasma sample sets were identified. These identified glycans were compared to the N-linked glycans cleaved from a pooled human plasma sample and all were found to be in common. The intra- and inter-individual variability for the plasma N-linked glycan $Hex_5HexNAc_5Fuc$ was calculated from all four birds and shown to be specific to individual birds. The nLC-LTQ–FT MS results, statistical analysis, and discussion of the dataset are provided.

2. Experimental

2.1. Materials

Peptide-N-glycosidase F (PNGase F; 2.5 mU/μL) was purchased from Prozyme (San Leandro, CA). Formic acid, trifluoracetic acid (TFA), ammonium acetate, lacto-N-difucohexaose I (LND), lacto-N-fucopentose (LNF), maltoheptaose, β-mercaptoethanol, and sodium dodecyl sulfate were purchased from Sigma Aldrich (St Louis, MO). Pooled human plasma was purchased from Innovative Research (Novi, MI). Graphitized solid-phase extraction cartridges (Part Number 210101) were purchased from Alltech (Deerfield, IL). HPLC grade acetonitrile and water were purchased from Burdick & Jackson (Muskegon, MI). Nitrogen (99.98%) and LTQ helium bath gas (99.999%) were obtained from MWSC High Purity Gases (Raleigh, NC).

2.2. Methods

The glycan cleavage method was previously described in detail by Bereman et al. [49] and is summarized on the right side Fig. 1. The four birds were Normal 1 (bird i.d.# 612W), Normal 2 (bird i.d.# 646W), EOC (bird i.d.# 666B), and EOC/OVD (bird i.d.# 621W). The denaturing solutions consisting of 1 M β-mercaptoethanol and 2% (w/w) sodium dodecylsulfate were made from stock solutions. The sample preparation process can be summarized by the following steps: denaturation, glycan release, solid-phase extraction, and reconstitution/dilution for nanoLC–MS.

2.2.1. Denaturation

Briefly, 50 μL of chicken plasma was lyophilized for about an hour at 35 °C. To this, 250 μL of 50 mM Tris HCL buffer (pH 7.5) was added and the samples were vortexed. 28 μL of 2% SDS/1 M β-mercaptoethanol denaturing solution was then added followed by centrifugation, vortexing and heating in a water bath (95 °C) for 5 min. The samples were then placed on the lab bench and cooled to room temperature (~20 min).

2.2.2. Glycan release

5 μL of enzyme solution (12.5 mU PNGase F) was added to each sample, followed by vortexing and centrifugation. The samples were incubated at 37 °C for 18 h. To quench the enzymatic activity, 500 μL of 99.9% water/0.1% TFA was added to each sample.

2.2.3. Solid-phase extraction

Nonporous graphitized carbon extraction columns were conditioned with (a) 14 mL of 99.9% water/0.1% TFA, (b) 7 mL of 80% ACN/20% water/0.05% TFA, (c) 14 mL of 99.9% water/0.1% TFA. Samples were loaded onto the column bed, and the sample vials were rinsed and vortexed twice with 500 μL of wash solution to ensure complete loading of sample. Loaded samples were washed with
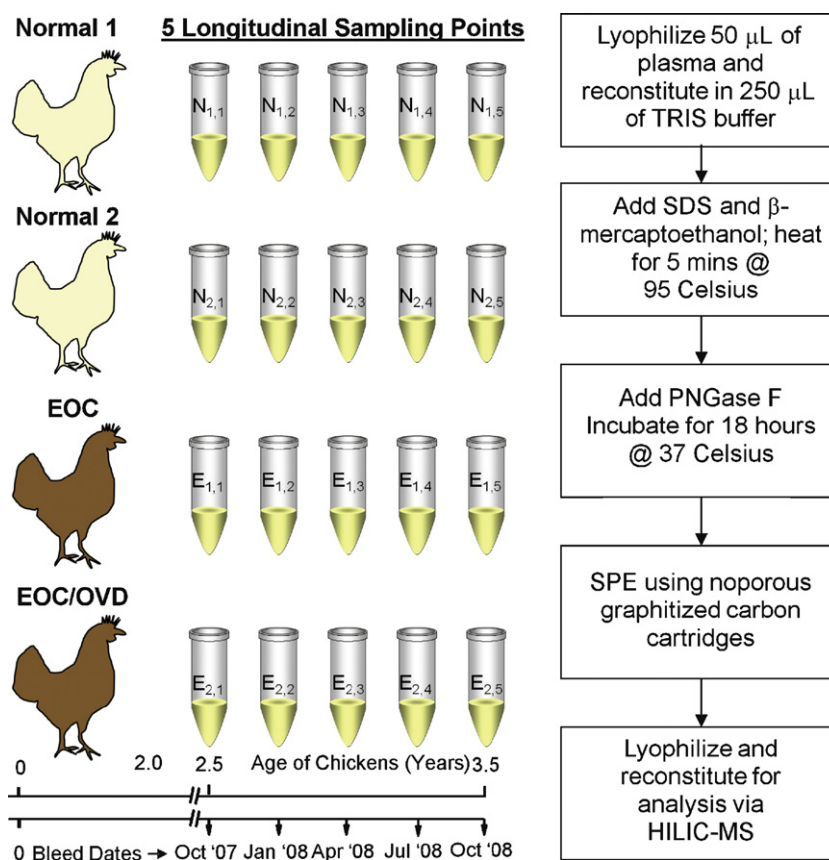
Fig. 1. Longitudinal sample procurement and processing method to investigate the *N*-linked plasma glycome in the avian model of epithelial ovarian cancer.

50 mL of 99.9% water/0.1% TFA. Elution of the samples was performed by washing the column bed with 25% ACN/75% water/0.1% TFA and collecting the eluent in a 1.5 mL eppendorf tube. Four elutions were collected for each sample under identical conditions.

2.2.4. Sample preparation for nanoLC-LTQ-FT MS

The eluent was lyophilized for ∼4 h at 35 °C. Samples were reconstituted by addition of 10 μL water, followed by vortexing, centrifugation, and combination of the four elution fractions for each sample. Of each sample, 5 μL was aliquoted to a sample vial to be analyzed by nanoLC–MS. To this vial, 100 μL of internal standard solution (0.4 μM each) containing lacto-N-difucohexaose I (LND), lacto-N-fucopentose (LNF), and maltoheptaose, was added. Each sample was further diluted by adding 100 μL of mobile phase B (80% ACN/20% water). The resulting solution was vortexed and added to a low-volume LC vial.

2.2.5. Nano-flow liquid chromatography

An Eksigent nanoLC-2D system (Dublin, CA) was used under conditions for hydrophilic interaction liquid chromatography (HILIC) in these experiments [50]. Mobile phase A was 50 mM ammonium acetate (pH 4.5), and mobile phase B was 100% acetonitrile. HILIC chromatography was performed over a continuous bed column, known as the vented column configuration with a "dummy" column [51]. The "dummy" column provides a continuous backpressure during valve switching. The nanoLC method used herein has been previously described [52]. The trap and analytical and dummy columns were slurry packed in house with TSK-Gel Amide80 stationary phase (Tosoh Biosciences, San Francisco, CA) to lengths of 5, 10 and 15 cm, respectively. The trap and dummy columns were packed into IntegraFrit capillaries (New Objective, Woburn, MA) and the analytical column was packed into PicoFrit

capillary column with a 15 μm I.D. tip (New Objective, Woburn, MA).

4 μL of sample were injected into a 10 μL loop and washed onto the trap column at a flow rate of 2 μL/min (80% ACN). While the loading pump was washing over the trap column, the nano-flow pumps were equilibrated with the dummy column such that minimal pressure fluctuations would occur during valve switching. The loaded sample was washed with 10 trap column volumes prior to the switching of the 10-port valve (VICI, Houston, TX) in-line with the gradient flow at 500 nL/min. At this time data collection was initiated. After 3 min, mobile phase A was increased from 20% to 60% over 37 min, and remained at 60% for an additional 5 min prior to decreasing to 20% over 5 min. The system was then allowed to re-equilibrate for 10 min resulting in total run time of 60 min.

2.2.6. LTQ-FT MS

All mass spectra were acquired on a hybrid LTQ-FT-ICR mass spectrometer (Thermo Fisher, San Jose, CA) equipped with an Oxford Instruments actively shielded 7T superconducting magnet (Concord, MA) operating in positive ion, FT mode. The MS heated metal capillary temperature was held constant at 250 °C. A 2 kV potential was applied to a zero dead volume union to achieve electrospray ionization. Resolving power was set to $100,000_{FWHM}$ at m/z 400; one precursor scan and up to four MS/MS events were recorded. Dynamic exclusion was enabled with 120 s duration. The AGC limits for the FT and LTQ were 1×10^6 for a maximum of 1 s and 1×10^4 for a maximum of 400 ms, respectively. The MS heated metal capillary was set to 42 V, and the tube lens was set to 120 V. Identification of glycans was aided by the use of OSCAL software (personal communication; Lebrilla and coworkers). Peak integration was performed using Xcalibur 2.0.7. Interrogation of glycan data was also aided by SimGlycan
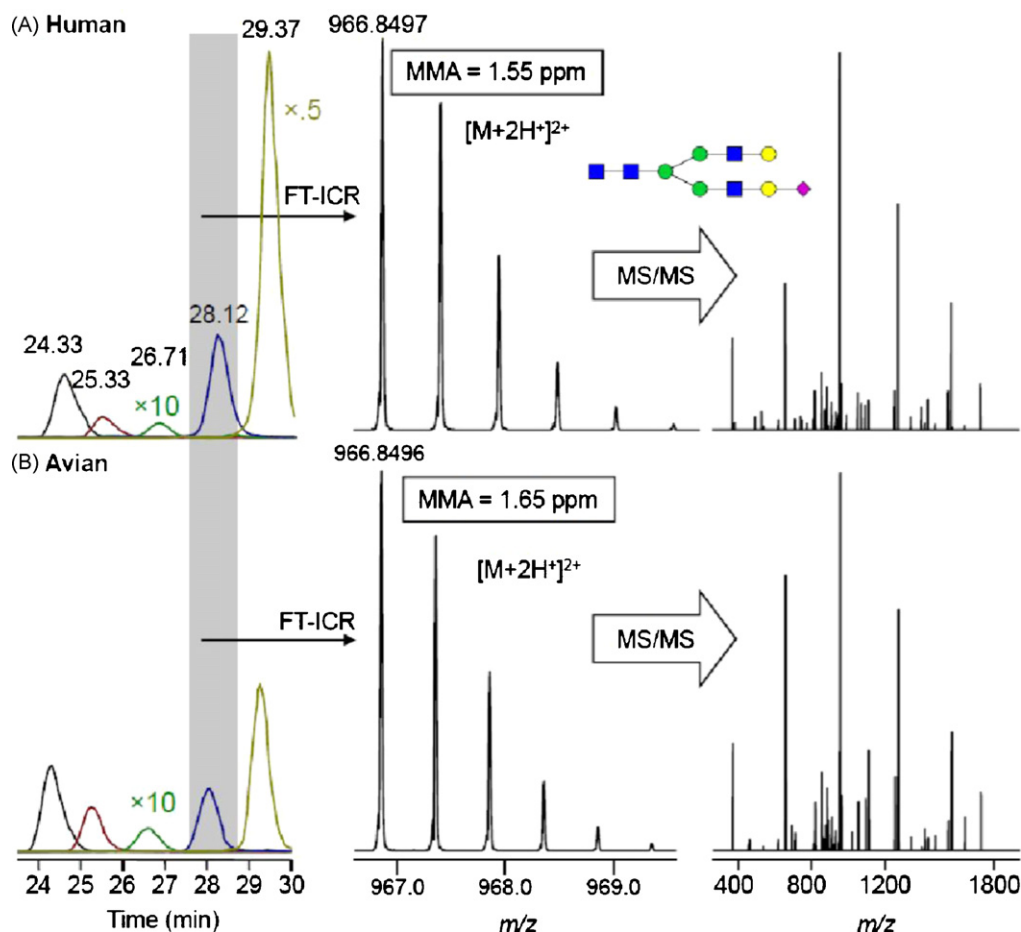
Fig. 2. Comparison of five selected *N*-linked glycans from human plasma (A), and avian plasma (B). Similar retention times are observed, along with comparable mass measurement accuracy and MS/MS spectra. This data supports the hypothesis that the same compositions are observed in both species. The composition and detected *m/z* values are provided in the text. The following symbols are used in the schematics: N-acetylglucosamine (blue square), mannose (green circle), galactose (yellow circle), and sialic acid (purple diamond). (For interpretation of the references to color in this figure legend, the reader is referred to the web version of the article.)

2.7 (http://www.premierbiosoft.com), and GlycoWorkbench version 1.1 which is part of the European Carbohydrates DataBase project (http://www.eurocarbdb.org/) [53].

3. Results and discussion

A major limitation of biomarker discovery using the clinical samples from human EOC patients is that these studies are typically limited to single-time point analysis due in large part to very low incidence of the disease and the logistical complexities of obtaining multiple samples from a human subject. The chicken model allows us to have a large cohort of animals with a well-defined genetic and environmental (*e.g.*, diet, lifestyle, exercise, etc.) background that can be sampled longitudinally and then subsequently obtain matched tissue specimens. Thus, as the chicken progresses from normal/healthy to disease, changes in the *N*-linked glycome can be correlated to the disease. This experimental strategy results in significant and quantitative information as to how the *N*-linked glycome is altered by EOC.

The experimental workflow for this study is outlined in Fig. 1. The goal of this research strategy is to determine the biochemical variability with respect to the integrated glycan peak area within (intra) and between (inter) normal, EOC, and EOC + other cancer samples; this topic has been discussed in the literature for over half of a century [54–57]. Plasma samples were obtained from chickens over a one-year period at three-month intervals start-

ing at 2.5 years of age. The birds selected for this study included two normal (healthy) birds, one bird with early-stage EOC (tumor confined to the ovary), and one bird with EOC or oviductal cancer (OVD). The two birds with cancer were evaluated by a board certified veterinary pathologist and confirmed to be adenocarcinomas. When neoplastic lesions are found on both the ovary and oviduct in a chicken and then both confirmed through pathology to be adenocarcinomas, there is no present way to determine the tissue of origin. Thus, the bird with adenocarcinomas on both the ovary and oviduct is denoted "EOC/OVD". The nLC-LTQ–FT MS analysis of the longitudinal plasma samples from the four birds allowed for a differential analysis between normal/healthy and EOC. The data presented in this report represents an initial use of quantitative mass spectrometry-based technology to measure the intra- and inter-individuality of *N*-linked glycans in plasma. The framework of this study will serve as a foundation for ongoing studies in our laboratory involving larger numbers of birds combined with matched ovarian tissue specimens.

A human plasma control sample was processed and analyzed in parallel with the 4 longitudinal chicken sample sets to compare both the structures and the relative intensities of the *N*-linked glycans measured by nHILIC–LTQ–FT MS. The results from this comparison are shown in Fig. 2. As an example of the overlap observed between human (Fig. 2A) and chicken (Fig. 2B) samples, five extracted ion chromatograms are plotted. The five extracted ion chromatograms represent the following glycan compositions with their *m/z* values in ascending chronological order

Table 1

Identified N-glycans from avian plasma. All glycans have been previously identified and reported for human plasma. Many glycans were observed as $(M+2H^+)^{2+}$. The bolded N-glycans are further described in Fig. 2. The third column provides the 95% CI of the MMA while the final column provides the CI values for the retention times.

Composition	Theoretical $(M+1H)^{1+}$	$MMA_{average}$ (ppm)	95% CI ($n=4$)	$RT_{average}$ (min)	95% CI ($n=4$) (s)
$Hex_3HexNAc_2$	911.3350	0.52	1.38	20.14	15.23
$Hex4HexNAc_2$	1073.3878	0.98	0.55	22.78	8.48
$Hex_3HexNAc_3$	1114.4150	1.62	0.37	21.86	19.04
$Hex_5HexNAc_2$	**1235.4410**	**1.78**	**0.11**	**24.94**	**15.13**
$Hex4HexNAc_3$	1276.4670	1.08	0.95	24.07	15.55
$Hex_3HexNAc_4$	1317.4940	1.31	0.82	23.16	13.07
$Hex_6HexNAc_2$	**1397.4940**	**1.90**	**0.29**	**26.71**	**17.09**
$Hex_3H\,exNAc_3NeuAc_1$	1405.5100	0.73	1.07	24.55	15.37
$Hex_5HexNAc_3$	1438.5176	0.36	1.68	25.75	8.62
$Hex_3HexNAc_4Fuc_1$	1463.5520	0.02	1.11	25.75	13.07
$Hex_4HexNAc_4$	1479.5470	0.95	1.14	25.31	5.45
$Hex_3HexNAc_5$	1520.5732	0.66	0.45	23.83	5.88
$Hex_6HexNAc_3$	1600.5728	0.47	0.71	27.51	9.08
$Hex_4HexNAc_4Fuc_1$	1625.6050	0.34	0.68	25.41	4.83
$Hex_5HexNAc_4$	1641.5994	0.85	0.57	26.70	13.68
$Hex_3HexNAc_5Fuc_1$	1666.6310	1.41	0.29	24.33	6.67
$Hex_4HexNAc_5$	1682.6260	1.16	0.32	25.33	7.01
$Hex_5HexNAc_3NeuAc_1$	**1729.6154**	**0.92**	**0.40**	**27.57**	**14.12**
$Hex_4HexNAc_4NeuAc_1$	1770.6520	0.79	0.44	26.74	8.00
$Hex_5HexNAc_4Fuc_1$	1787.6573	0.22	1.71	27.32	16.49
$Hex_4HexNAc_5Fuc_1$	1828.6839	1.37	0.22	25.84	14.07
$Hex_5HexNAc_5$	1844.6788	1.27	0.26	26.85	7.65
$Hex_6HexNAc_3NeuAc_1$	1891.6682	0.63	1.22	28.85	6.75
$Hex_5HexNAc_4NeuAc_1$	**1932.6848**	**1.60**	**0.16**	**28.12**	**6.86**
$Hex_5HexNAc_5Fuc_1$	1990.7367	1.10	0.23	27.33	14.55
$Hex_4HexNAc_4Fuc_1NeuAc_1$	2078.7527	0.75	0.78	28.41	4.58
$Hex_4HexNAc_5Fuc_1NeuAc_1$	2119.7793	0.40	0.54	27.58	15.79
$Hex_5HexNAc_5NeuAc_1$	2135.7742	1.45	0.56	28.31	11.19
$Hex_5HexNAc_4NeuAc_2$	2223.7902	1.91	0.14	29.37	8.13
$Hex_5HexNAc_5Fuc_1NeuAc_1$	2281.8321	1.38	0.47	28.71	9.74
$Hex_5HexNAc_5NeuAc_1$	2297.8270	0.33	1.65	29.30	13.59
$Hex_5HexNAc_4Fuc_1NeuAc_2$	2369.8481	1.58	0.54	29.64	7.67
$Hex_5HexNAc_5NeuAc_2$	2426.8696	0.95	1.18	29.50	8.43
$Hex_5HexNAc_5Fuc_1NeuAc_2$	2572.9275	1.28	0.51	29.75	8.15
$Hex_6HexNAc_5NeuAc_2$	2588.9224	1.08	0.22	30.55	13.34

(based on retention times): (1) $Hex_3HexNAc_5Fuc_1$ m/z 833.8193, (2) $Hex_4HexNAc_5$ m/z 841.8168, (3) $Hex_6HexNAc_2$ m/z 1397.4940, (4) $Hex_5HexNAc_4NeuAc_1$ m/z 966.8512, and (5) $Hex_5HexNAc_4NeuAc_2$ m/z 1112.3990. The gray column in Fig. 2 highlights a representative precursor ion found in both chicken and human plasma at the same retention time (within 1.5 s) with a charge state of 2^+ and similar mass measurement accuracy. In addition to the identical retention times and precursor ion mass accuracy, the fragmentation patterns for the human sample (Fig. 2A) and the chicken sample (Fig. 2B) have several similar prominent spectral features. Furthermore, every N-glycan composition identified in the chicken sample by combined accurate mass and MS/MS has been identified in human plasma. These results are promising with regard to translating insights from longitudinal chicken plasma to human EOC in the form of candidate biomarkers. Having established that the human and chicken plasma N-linked glycomes have significant compositional similarities, longitudinal plasma samples from birds across a spectrum of health and disease states can be interrogated in the context of EOC biomarker discovery and its translation to humans.

A list of all 35 N-linked glycan compositions identified in this study from chicken plasma is given in Table 1. These encompass several characteristic N-glycans including high mannose, complex and hybrid structures. These identified species were composed of a number of combinations of hexose, N-acetylhexosamine, fucose and sialic acid. Predominately $(M+H^+)^{1+}$ and $(M+2H^+)^{2+}$ along with some ammonium adducted species were detected. In the case of ammonium adducted species, both the protonated and ammonium adducted species peak areas were integrated. Accurate mass and MS/MS data for the N-linked glycans highlighted in Table 1 are further described in Fig. 3.

Fig. 3 highlights three major classes N-glycan structures that were observed. The precursor mass spectra shown on the left of Fig. 3 were measured in the FT-ICR cell to provide high resolving power and mass measurement accuracy (MMA) of the N-linked glycan species. Fig. 3A ($Hex_5HexNAc_2$) and Fig. 3B ($Hex_6HexNAc_2$) represents two high mannose structures that were identified from precursor MS (left) and MS/MS (right) data. The intact species detected were 1^+ and sequencing information from this precursor was obtained in the MS/MS spectrum. Assigned structures for each N-linked glycan are shown in the insets of their respective MS data. Fig. 3C and D represents MS and MS/MS data from the 2+ charge states of a hybrid glycan structure ($Hex_5HexNAc_3NeuAc_1$) and a complex structure ($Hex_5HexNAc_4NeuAc_1$).

Fig. 4 shows the integrated peak areas of an N-linked glycan (composition $Hex_5HexNAc_5Fuc$) in triplicate for the two normal (Normal 1 & Normal 2), the early-stage EOC, and the EOC/OVD chickens as a function of plasma sampling time point. From this experimental design a comparison of the integrated peak areas as a function of time can be made. From the upper left column, the Normal 1 bird has a consistently higher level of the $Hex_5HexNAc_5Fuc$ glycan compared with EOC. Interestingly, the $Hex_5HexNAc_5Fuc$ level in the Normal 1 bird stays relatively constant yet the EOC bird steadily increases over the same time period. The data plotted in the lower left column in Fig. 4 includes the $Hex_5HexNAc_5Fuc$ levels in plasma for the Normal 2 and EOC/OVD birds as a function of time. Unlike the Normal 1 and EOC birds, the $Hex_5HexNAc_5Fuc$ levels for the EOC/OVD bird are consistently higher than the Normal 2 bird for the one-year period. Furthermore, the $Hex_5HexNAc_5Fuc$ levels for the EOC/OVD remain relatively constant over the one-year period in comparison to the EOC bird. The gray columns provide a graphical representation of the intra- and inter-individual variability for the
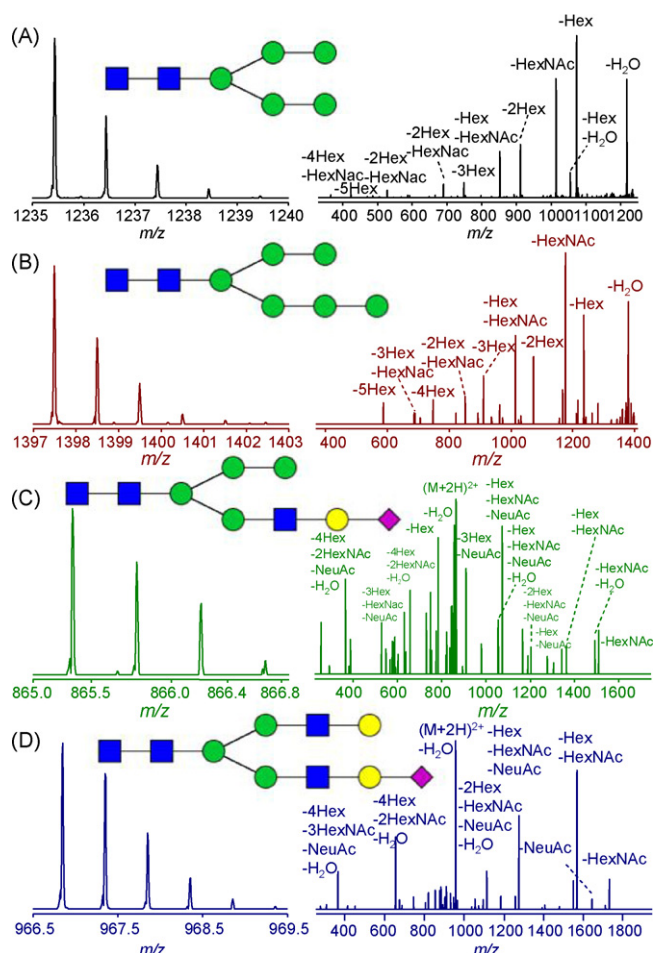
Fig. 3. Assigned structures and representative MS and tandem MS spectra of four N-glycans identified in this study. (A and B) High mannose structures observed as $(M+H^+)^{1+}$ intact ions. Their tandem MS spectra show characteristic fragmentation with extensive loss of both hexose and HexNAc. (C) A hybrid structure and the tandem MS spectrum reveal losses of NeuAc, hexose and HexNAc. (D) A complex structure and has characteristic losses of NeuAc, hexose and HexNAc. The following symbols are used in the schematics: N-acetylglucosamine (blue square), mannose (green circle), galactose (yellow circle), and sialic acid (purple diamond). (For interpretation of the references to color in this figure legend, the reader is referred to the web version of the article.)

Fig. 4. Data across the longitudinal study for a fucosylated N-glycan $Hex_5HexNAc_5Fuc_1$ m/z 995.87 $(M+2H^+)^{2+}$. The detected peak area for each sample is plotted as a function of the sample procurement time point. The longitudinal trends based on peak area are plotted for each chicken as follows: normal 1 (upper left, pink squares), EOC (upper left, black circles), EOC/OVD (lower left, red triangles), normal 2 (lower left, blue diamonds). There are major differences between distinct normal and EOC & EOC/OVD chickens. The inter-individuality of the range between the normal samples is greater than the inter-individuality of the EOC samples. These data emphasize the need for longitudinal sampling strategies to determine intra-individual variability for normal and disease samples. (For interpretation of the references to color in this figure legend, the reader is referred to the web version of the article.)

4 datasets. The raw data in the gray columns are given in Table 2. In the middle column, the following data is reported: the intra-normal variability – how does this N-linked glycan change during the course of aging in a normal chicken? The box plot in the middle column shows a 95% confidence interval range of 1.22×10^7 for Normal 1 and a smaller 95% confidence interval range of 3.92×10^6 for Normal 2 indicating the normal range for fluctuations in the peak area of this glycan. Additionally, the intra-EOC variability is reported – how does this N-linked glycan change during progres-

sion towards EOC? The 95% confidence interval range shown in the box plot for EOC is 2.49×10^7 and the 95% confidence interval range for EOC/OVD is 9.26×10^6. The 95% confidence interval for EOC is larger than either of the Normal ranges, and each of the EOC ranges is larger than the corresponding Normal individual utilized in this comparison. Considering both the upward trend and the larger 95% confidence interval, this glycan may be suggestive of the onset of disease for EOC. The right gray column of Fig. 4 shows the inter-normal variability – how does the integrated N-linked glycan peak area differ between normal chickens as they age? The 95% confidence interval range for Normal chickens is 6.76×10^7. The inter-EOC & EOC/OVD variability is also presented – how does the integrated N-linked glycan peak area differ between chickens as they progress to disease? The 95% confidence interval range for EOC & EOC/OVD chickens is 1.03×10^7.

These data are very interesting as they show the normal range for this N-glycan as being much larger than that of the diseased population (see Table 2). From these data, it would be clear that this

Table 2

Calculated median and 95% confidence interval values for the integrated peak areas of the $Hex_5HexNAc_5Fuc$ intra-individuality and inter-individuality plots shown in Fig. 3.

	#	Min ($\times 10^7$)	Median ($\times 10^7$)	95% CI ($\times 10^7$)	Max
(A) Intra-individuality					
Normal 1	15	10.3	10.9	10.6–11.8	13.3
EOC	15	3.8	5.3	4.5–7.0	8.6
(B) Intra-individuality					
Normal 2	15	3.3	4.0	3.9–4.2	5.0
EOC/OVD	15	4.9	6.0	5.5–6.4	6.6
(C) Inter-individuality					
Normal	30	3.3	7.7	4.0–10.8	13.3
EOC & EOC/OVD	30	3.8	5.6	5.3–6.3	8.6

N-linked glycan would not be effective for this population, however by looking at individual ranges, it becomes evident that the upward trend across time for EOC would make it diagnostic for that individual assuming the onset of EOC is indicative of the trending data. In other words, the mean $Hex_5HexNAc_5Fuc$ levels in plasma and their corresponding variabilities over time are specific to individual chickens. Yet, if the EOC bird is indicative of early-stage EOC with regards to onset time and the $Hex_5HexNAc_5Fuc$ levels are related to the onset of disease, this example clearly underscores the value of longitudinal sampling. For example, if single-time point samples were collected from the Normal 1 and EOC birds at "Longitudinal Sample Point 5", the differences would suggest a slight down-regulation of $Hex_5HexNAc_5Fuc$ in EOC compared with Normal 1. However, the longitudinal data for EOC clearly shows the $Hex_5HexNAc_5Fuc$ levels trending up (*i.e.*, up-regulation). Thus, the direction of glycan regulation would be mis-interpreted if these two birds were indicative of a population of birds at time point "5".

If we are to assume that $Hex_5HexNAc_5Fuc$ levels are indicative of EOC onset, how can the EOC/OVD data be explained where the abundances are relatively constant over the one-year period? Three explanations are considered here. First, $Hex_5HexNAc_5Fuc$ levels may have nothing to do with the onset of EOC which would be borne out of a larger-scale study with more birds. A second explanation could be that the EOC/OVD bird's tumor originated in the oviduct and that $Hex_5HexNAc_5Fuc$ is only specific to adenocarcinomas of the ovary. A third explanation could be that if the EOC/OVD tumor originated in the ovary, the onset of EOC may have occurred prior to 2.5 years of age. The onset and progression of cancer are believed to be the result of multiple somatic gene mutations (4–6) accumulated over time [58,59]. Thus, if $Hex_5HexNAc_5Fuc$ is indicative of EOC, the one-year widow between 2.5 and 3.5 years of age may be a homeostatic plateau resulting from an earlier increase. The point of these speculative scenarios is to illustrate the inherent value of longitudinal samples in establishing personalized reference ranges for multiple glycans as a function of health and disease. By studying multiple glycan species over time, biomarkers may reveal themselves in ways otherwise impossible with conventional single-time point approaches.

4. Conclusions

The *N*-linked glycomes from chickens and humans were characterized by nLC-LTQ–FT MS and found to be similar with regard to the compositions of identified species. A total of 35 plasma *N*-linked glycans were identified from chickens in this study and all of these have been previously found in humans [49]. The similarity of the *N*-linked glycome is yet another piece of molecular-level evidence supporting the similarities between EOC in chickens versus humans. Quantitative changes of the *N*-linked glycome from 4 chickens were studied as a function of time using nLC-LTQ–FT MS. The plasma levels of $Hex_5HexNAc_5Fuc$ were shown to be specific to each of the 4 chickens. The levels of $Hex_5HexNAc_5Fuc$ in the two normal birds were relatively constant for samples collected over the one-year period but the inter-individual means were different by almost 3-fold. The increasing $Hex_5HexNAc_5Fuc$ levels in the EOC bird provided an important illustration of the power of longitudinal sampling. Although the levels in the EOC bird increased by approximately 2-fold over the one-year period, the final measured abundance did not exceed the intra-individual mean for the Normal 1 bird. In other words, comparative analysis of time point "5" for the Normal 1 and EOC birds would have suggested a down-regulation of $Hex_5HexNAc_5Fuc$ as a result of EOC onset. The strategy described in this study provides a foundation for studying the onset of EOC as a function of time to establish "personalized" reference ranges and ultimately novel glycan biomarkers for early-stage EOC.

5. Supporting Information

All of the nLC-LTQ–FT MS/MS data files associated with this manuscript may be downloaded from the ProteomeCommons.org Tranche network using the following hash: xNrry + SE2MHkMBy7EH4g29okzO2ZL0mmq1MPVd1MYC/iXPwVAe CUMW/PN + A3GIWw/dZJa8uoN + SxFmI8WnlY + JrKqHUAAAAAA ACgew==.

Acknowledgements

References

[1] R. Grummer, Animal models in endometriosis research, Human Reproduction Update 12 (5) (2006) 641–649.
[2] B.W. Calnek, Chicken neoplasia – a model for cancer-research, British Poultry Science 33 (1) (1992) 3–16.
[3] G. Wick, L. Andersson, K. Hala, M.E. Gershwin, C. Selmi, G.F. Erf, S.J. Lamont, R. Sgonc, Avian Models with Spontaneous Autoimmune Diseases. Advances in Immunology, vol. 92, Elsevier, Academic Press Inc., San Diego, 2006, pp. 71–117.
[4] G.J. Lieschke, P.D. Currie, Animal models of human disease: zebrafish swim into view, Nature Reviews Genetics 8 (5) (2007) 353–367.
[5] M.J. Day, The canine model of dietary hypersensitivity, Proceedings of the Nutrition Society 64 (4) (2005) 458–464.
[6] S.T.A. Malik, R.G. Knowles, N. East, D. Lando, G. Stamp, F.R. Balkwill, Antitumor-activity of gamma-interferon in ascitic and solid tumor-models of human ovarian-cancer, Cancer Research 51 (24) (1991) 6643–6649.
[7] A.F. Cheung, M.J.P. DuPage, H.K. Dong, J.Z. Chen, T. Jacks, Regulated expression of a tumor-associated antigen reveals multiple levels of T-cell tolerance in a mouse model of lung cancer, Cancer Research 68 (22) (2008) 9459–9468.
[8] E. Bockamp, M. Maringer, C. Spangenberg, S. Fees, S. Fraser, L. Eshkind, F. Oesch, B. Zabel, Of mice and models: improved animal models for biomedical research, Physiological Genomics 11 (3) (2002) 115–132.
[9] R. Coico, D.S. Woodruff-Pak, Immunotherapy for Alzheimer's disease: harnessing our knowledge of T cell biology using a cholesterol-fed rabbit model, Journal of Alzheimers Disease 15 (4) (2008) 657–671.
[10] S.H. Yang, P.H. Cheng, H. Banta, K. Piotrowska-Nitsche, J.J. Yang, E.C.H. Cheng, B. Snyder, K. Larkin, J. Liu, J. Orkin, Z.H. Fang, Y. Smith, J. Bachevalier, S.M. Zola, S.H. Li, X.J. Li, A.W.S. Chan, Towards a transgenic model of Huntington's disease in a non-human primate, Nature 453 (7197) (2008) (921–U56).
[11] P.M. Conn, J.M. Bahr, Sourcebook of Models for Biomedical Research: The Chicken as a Model Organism, Humana Press Inc., Totowa, NJ, 2008.
[12] J.T. Casagrande, M.C. Pike, R.K. Ross, E.W. Louie, S. Roy, B.E. Henderson, Incessant ovulation and ovarian-cancer, Lancet 2 (8135) (1979) 170–172.
[13] C. Rodriguez-Burford, M.N. Barnes, W. Berry, E.E. Partridge, W.E. Grizzle, Immunohistochemical expression of molecular markers in an avian model: a potential model for preclinical evaluation of agents for ovarian cancer chemo-prevention, Gynecologic Oncology 81 (3) (2001) 373–379.
[14] E. Jackson, K. Anderson, C. Ashwell, J. Petitte, P.E. Mozdziak, CA125 expression in spontaneous ovarian adenocarcinomas from Laying Hens, Gynecologic Oncology 104 (1) (2007) 192–198.
[15] A.A. Hakim, C.P. Barry, H.J. Barnes, K.E. Anderson, J. Petitte, R. Whitaker, J.M. Lancaster, R.M. Wenham, D.K. Carver, J. Turbov, A. Berchuck, L. Kopelovich, G.C. Rodriguez, Ovarian adenocarcinomas in the Laying Hen and women share similar alterations in p53, ras, and HER-2/neu, Cancer Prevention Research 2 (2) (2009) 114–121.
[16] R. Apweiler, H. Hermjakob, N. Sharon, On the frequency of protein glycosylation, as deduced from analysis of the SWISS-PROT database, Biochimica Et Biophysica Acta-General Subjects 1473 (1) (1999) 4–8.
[17] A. Varki, Sialic acids in human health and disease, Trends in Molecular Medicine 14 (8) (2008) 351–360.
[18] M.V. Dwek, S.A. Brooks, Harnessing changes in cellular glycosylation in new cancer treatment strategies, Current Cancer Drug Targets 4 (5) (2004) 425–442.
[19] R. Peracaula, L. Royle, G. Tabares, G. Mallorqui-Fernandez, S. Barrabes, D.J. Harvey, R.A. Dwek, P.M. Rudd, R. de Llorens, Glycosylation of human pancreatic ribonuclease: differences between normal and tumor states, Glycobiology 13 (4) (2003) 227–244.
[20] Y.Y. Zhao, M. Takahashi, J.G. Gu, E. Miyoshi, A. Matsumoto, S. Kitazume, N. Taniguchi, Functional roles of N-glycans in cell signaling and cell adhesion in cancer, Cancer Science 99 (7) (2008) 1304–1310.
[21] O. Warburg, Uber den Stofwechsel der carcinomzelle, Klinische Wochenschrift Berliner 4 (1925) 534.
[22] H.C. Wu, E. Meezan, P.H. Black, P.W. Robbins, Comparative studies on carbohydrate-containing membrane components of normal and virus-

transformed mouse fibroblasts. I. Glucosamine-labeling patterns in 3t3 spontaneously transformed 3t3 and Sv-40-transformed 3t3 cells, Biochemistry 8 (6) (1969) 2509.

[23] I. Rostenberg, J. Guizarvazquez, R. Penaloza, Altered carbohydrate content of alpha-1-antitrypsin in patients with cancer, Journal of the National Cancer Institute 61 (4) (1978) 961–965.

[24] C.W. Gehrke, T.P. Waalkes, E. Borek, W.F. Swartz, T.F. Cole, K.C. Kuo, M. Abeloff, D.S. Ettinger, N. Rosenshein, R.C. Young, Quantitative gas–liquid-chromatography of neutral sugars in human-serum glycoproteins – fucose, mannose, and galactose as predictors in ovarian and small cell lung-carcinoma, Journal of Chromatography 162 (4) (1979) 507–528.

[25] R.C. Casey, T.R. Oegema, K.M. Skubitz, S.E. Pambuccian, S.M. Grindle, A.P.N. Skubitz, Cell membrane glycosylation mediates the adhesion, migration, and invasion of ovarian carcinoma cells, Clinical & Experimental Metastasis 20 (2) (2003) 143–152.

[26] J.W. Dennis, M. Granovsky, C.E. Warren, Protein glycosylation in development and disease, Bioessays 21 (5) (1999) 412–421.

[27] K.S. Lau, J.W. Dennis, N-glycans in cancer progression, Glycobiology 18 (10) (2008) 750–760.

[28] M.A. Hollingsworth, B.J. Swanson, Mucins in cancer: protection and control of the cell surface, Nature Reviews Cancer 4 (1) (2004) 45–60.

[29] S. Hakomori, Glycosylation defining cancer malignancy: new wine in an old bottle, Proceedings of the National Academy of Sciences of the United States of America 99 (16) (2002) 10231–10233.

[30] E. Gorelik, U. Galili, A. Raz, On the role of cell surface carbohydrates and their binding proteins (lectins) in tumor metastasis, Cancer and Metastasis Reviews 20 (3–4) (2001) 245–277.

[31] C.B. Lebrilla, H.J. An, The prospects of glycan biomarkers for the diagnosis of diseases, Molecular Biosystems 5 (1) (2009) 17–20.

[32] R. Peracaula, G. Tabares, L. Royle, D.J. Harvey, R.A. Dwek, P.M. Rudd, R. de Llorens, Altered glycosylation pattern allows the distinction between prostate-specific antigen (PSA) from normal and tumor origins, Glycobiology 13 (6) (2003) 457–470.

[33] Y.J. Kim, A. Varki, Perspectives on the significance of altered glycosylation of glycoproteins in cancer, Glycoconjugate Journal 14 (5) (1997) 569–576.

[34] D.H. Dube, C.R. Bertozzi, Glycans in cancer and inflammation. Potential for therapeutics and diagnostics, Nature Reviews Drug Discovery 4 (6) (2005) 477–488.

[35] J.W. Dennis, S. Laferte, C. Waghorne, M.L. Breitman, R.S. Kerbel, Beta-1-6 branching of asn-linked oligosaccharides is directly associated with metastasis, Science 236 (4801) (1987) 582–585.

[36] Z. Kyselova, Y. Mechref, M.M. Al Bataineh, L.E. Dobrolecki, R.J. Hickey, J. Vinson, C.J. Sweeney, M.V. Novotny, Alterations in the serum glycome due to metastatic prostate cancer, Journal of Proteome Research 6 (5) (2007) 1822–1832.

[37] M.L.A. de Leoz, H.J. An, S. Kronewitter, J. Kim, S. Beecroft, R. Vinall, S. Miyamoto, R.D. White, K.S. Lam, C. Lebrilla, Glycomic approach for potential biomarkers on prostate cancer: profiling of N-linked glycans in human sera and pRNS cell lines, Disease Markers 25 (4–5) (2008) 243–258.

[38] D. Isailovic, R.T. Kurulugama, M.D. Plasencia, S.T. Stokes, Z. Kyselova, R. Goldman, Y. Mechref, M.V. Novotny, D.E. Clemmer, Profiling of human serum glycans associated with liver cancer and cirrhosis by IMS–MS, Journal of Proteome Research 7 (3) (2008) 1109–1117.

[39] C. Kirmiz, B.S. Li, H.J. An, B.H. Clowers, H.K. Chew, K.S. Lam, A. Ferrige, R. Alecio, A.D. Borowsky, S. Sulaimon, C.B. Lebrilla, S. Miyamoto, A serum glycomics approach to breast cancer biomarkers, Molecular & Cellular Proteomics 6 (1) (2007) 43–55.

[40] Z. Kyselova, Y. Mechref, P. Kang, J.A. Goetz, L.E. Dobrolecki, G.W. Sledge, L. Schnaper, R.J. Hickey, L.H. Malkas, M.V. Novotny, Breast cancer diagnosis and prognosis through quantitative measurements of serum glycan profiles, Clinical Chemistry 54 (7) (2008) 1166–1175.

[41] H.J. An, S. Miyamoto, K.S. Lancaster, C. Kirmiz, B.S. Li, K.S. Lam, G.S. Leiserowitz, C.B. Lebrilla, Profiling of glycans in serum for the discovery of potential biomarkers for ovarian cancer, Journal of Proteome Research 5 (7) (2006) 1626–1635.

[42] B.S. Li, H.J. An, C. Kirmiz, C.B. Lebrilla, K.S. Lam, S. Miyamoto, Glycoproteomic analyses of ovarian cancer cell lines and sera from ovarian cancer patients show distinct glycosylation changes in individual proteins, Journal of Proteome Research 7 (9) (2008) 3776–3788.

[43] N.K. Wong, R.L. Easton, M. Panico, M. Sutton-Smith, J.C. Morrison, F.A. Lattanzio, H.R. Morris, G.F. Clark, A. Dell, M.S. Patankar, Characterization of the oligosaccharides associated with the human ovarian tumor marker CA125, Journal of Biological Chemistry 278 (31) (2003) 28619–28634.

[44] K.E. Krueger, S. Srivastava, Posttranslational protein modifications – current implications for cancer detection, prevention, and therapeutics, Molecular and Cellular Proteomics 5 (10) (2006) 1799–1810.

[45] T.S. Raju, J.B. Briggs, S.M. Borge, A.J.S. Jones, Species-specific variation in glycosylation of IgG: evidence for the species-specific sialylation and branch-specific galactosylation and importance for engineering recombinant glycoprotein therapeutics, Glycobiology 10 (5) (2000) 477–486.

[46] K.W. Koles, R. McDowell, S.P. Rose, Glycan analysis of the chicken synaptic plasma membrane glycoproteins – a major synaptic N-glycan carries the lewisx determinant, International Journal of Biological Science 1 (2005) 126–134.

[47] I.L. Tutykhina, O.A. Bezborodova, M.M. Shmarov, D.Y. Logunov, G.L. Neugodova, E.R. Nemtsova, B.S. Naroditsky, R.L. Yakubovskaya, A.L. Gintsburg, Production of recombinant human lactoferrin in the allantoic fluid of embryonated chicken eggs and its characteristics, Protein Expression and Purification 65 (1) (2009) 100–107.

[48] C.M. Martersteck, N.L. Kedersha, D.A. Drapp, T.G. Tsui, K.J. Colley, Unique alpha 2,8-polysialylated glycoproteins in breast cancer and leukemia cells, Glycobiology 6 (3) (1996) 289–301.

[49] M.S. Bereman, D.D. Young, A. Deiters, D.C. Muddiman, Development of a robust and high throughput method for profiling N-linked glycans derived from plasma glycoproteins by NanoLC–FTICR mass spectrometry, Journal of Proteome Research 8 (7) (2009) 3764–3770.

[50] A.J. Alpert, Hydrophilic-interaction chromatography for the separation of peptides, nucleic-acids and other polar compounds, Journal of Chromatography 499 (1990) 177–196.

[51] G.L. Andrews, C.M. Shuford, J.C. Burnett, A.M. Hawkridge, D.C. Muddiman, Coupling of a vented column with splitless nanoRPLC–ESI-MS for the improved separation and detection of brain natriuretic peptide-32 and its proteolytic peptides, Journal of Chromatography B-Analytical Technologies in the Biomedical and Life Sciences 877 (10) (2009) 948–954.

[52] M.S. Bereman, T.I. Williams, D.C. Muddiman, Development of a nanoLC LTQ orbitrap mass spectrometric method for profiling glycans derived from plasma from healthy, benign tumor control, and epithelial ovarian cancer patients, Analytical Chemistry 81 (3) (2009) 1130–1136.

[53] A. Ceroni, K. Maass, H. Geyer, R. Geyer, A. Dell, S.M. Haslam, Glycoworkbench: a tool for the computer-assisted annotation of mass spectra of glycans, Journal of Proteome Research 7 (4) (2008) 1650–1659.

[54] R.J. Williams, Biochemical Individuality: The Basis for the Genetotrophic Concept, John Wiley & Sons, 1956.

[55] A.J. Schneider, Some thoughts on normal, or standard, values in clinical medicine, Pediatrics 26 (1960) 973–984.

[56] E.K. Harris, Effects of intraindividual and interindividual variation on appropriate use of normal ranges, Clinical Chemistry 20 (12) (1974) 1535–1542.

[57] A.M. Hawkridge, D.C. Muddiman, Mass spectrometry-based biomarker discovery: toward a global proteome index of individuality, Annual Review of Analytical Chemistry 2 (2009), 13.1–13.13.

[58] W.C. Hahn, R.A. Weinberg, Modelling the molecular circuitry of cancer, Nature Reviews Cancer 2 (5) (2002) 331–341.

[59] D. Hanahan, R.A. Weinberg, Hallmarks of cancer, Cell 100 (2000) 57–70.